Published in final edited form as:
Neuron. 2012 January 12; 73(1): 49–63. doi:10.1016/j.neuron.2011.10.029.

Otic Mesenchyme Cells Regulate Spiral Ganglion Axon Fasciculation through a Pou3f4/EphA4 Signaling Pathway

Thomas M. Coate[1], **Steven Raft**[2], **Xiumei Zhao**[3], **Aimee K. Ryan**[4], **E. Bryan Crenshaw III**[5], and **Matthew W. Kelley**[1]

[1]Laboratory of Cochlear Development, National Institute on Deafness and Other Communication Disorders, National Institutes of Health; Bethesda, MD 20892; USA

[2]Sensory Cell Regeneration and Development Section, National Institute on Deafness and Other Communication Disorders, National Institutes of Health; Bethesda, MD 20892; USA

[3]Department of Biology, Georgetown University, Washington, D.C. 20057; USA

[4]Department of Pediatrics, McGill University; Research Institute of the McGill University Health Centre; Montreal, Quebec, Canada, H3A 2T5

[5]Children's Hospital of Philadelphia, University of Pennsylvania; Philadelphia, PA 19104; USA

SUMMARY

Peripheral axons from auditory spiral ganglion neurons (SGNs) form an elaborate series of radially and spirally oriented projections that interpret complex aspects of the auditory environment. However, the developmental processes that shape these axon tracts are largely unknown. Radial bundles are comprised of dense SGN fascicles that project through otic mesenchyme to form synapses within the cochlea. Here, we show that radial bundle fasciculation and synapse formation are disrupted when *Pou3f4* (DFNX2) is deleted from otic mesenchyme. Further, we demonstrate that Pou3f4 binds to and directly regulates expression of *Epha4*, that *Epha4*$^{-/-}$ mice present similar SGN defects, and that exogenous EphA4 promotes SGN fasciculation in the absence of Pou3f4. Finally, *Efnb2* deletion in SGNs leads to similar fasciculation defects, suggesting that ephrin-B2/EphA4 interactions are critical during this process. These results indicate a model whereby Pou3f4 in the otic mesenchyme establishes an Eph/ephrin-mediated fasciculation signal that promotes inner radial bundle formation.

INTRODUCTION

Hearing depends on hair cell-mediated conversion of sound stimuli into electrochemical information that is then relayed to the brain via spiral ganglion neurons (SGNs), a cluster of bipolar afferent neurons that parallel the medial surface of the cochlear coil. While considerable research has been conducted on the patterning of the hair cells and support cells within the cochlea (Driver and Kelley, 2009; Kelley, 2006; Puligilla and Kelley, 2009), relatively little work has focused on mechanisms that control the patterning, migration, and outgrowth of the SGNs (reviewed in Appler and Goodrich, 2011). As essential regulators of

Author for correspondence: coatet@nidcd.nih.gov; (301) 435-8074 (phone), (301) 480-3001 (fax)..

Please see SUPPLEMENTARY EXPERIMENTAL PROCEDURES for lists of the antibodies, *in situ* hybridization probes, qPCR primers, the quantification methods used in the study, and a description of the microarray that identified *Epha4*.

auditory information, a better understanding of how these processes occur within SGNs will enhance our understanding of auditory function, as well as how these neurons might be reformed in cases of deafness.

During development, immature proliferating neuroblasts delaminate from the otocyst (Ruben, 1967), and migrate to form a dense ganglion along the medial side of the inner ear epithelium. As development continues, developing SGNs extend peripheral axons through the surrounding (otic) mesenchyme cells (Carney and Silver, 1983) and subsequently penetrate the cochlear epithelium to form glutamate-responsive ribbon-type synapses with inner and outer hair cells (Smith, 1961). During this process, SGN axons form a series of dense fascicles, referred to as “inner radial bundles,” each of which contains fibers with similar frequency tuning. Groundbreaking work has begun to delineate the regulatory networks that establish the circuitry between the cochlea and CNS (Koundakjian et al., 2007), however specific mechanisms regulating SGN development patterning are unknown.

The POU-domain (Pit1-Oct1/2-unc86) proteins are a phylogenetically conserved family of transcription factors with diverse DNA binding affinities and a wide range of developmental functions (Phillips and Luisi, 2000; Ryan and Rosenfeld, 1997). Mutations in *POU3F4/Pou3f4*, located on the X-chromosome, cause deafness in humans (DFNX2) and mice (Kandpal et al., 1996; Minowa et al., 1999). Expression studies indicate that Pou3f4 expression is restricted to otic mesenchyme cells with limited or no expression in the hair cells or SGNs (Minowa et al., 1999; Phippard et al., 1998; Samadi et al., 2005). Consistent with this, the cochlear sensory epithelium (organ of Corti), which includes hair cells and supporting cells, appears normal in *Pou3f4*$^{-/-}$ mice. However, the cochlear duct has been described as dysplastic with a moderate length reduction, possibly owing to disorganization and altered morphology of otic mesenchyme cells (Minowa et al., 1999; Phippard et al., 1999). Considering the intimate relationship between developing SGNs and otic mesenchyme, defects in aspects of SGN formation in the absence of Pou3f4 seemed possible.

Any effects of Pou3f4 on SGN formation would most likely be indirect and therefore mediated by other factors. In particular, Eph receptors, the largest family of vertebrate receptor tyrosine kinases, are known to interact with ephrin ligands to generate both “forward” and “reverse” signals and have been linked extensively with axon guidance (Coate et al., 2009; Huai and Drescher, 2001; Pasquale, 2005; Wilkinson, 2001). While several studies have documented the presence of Ephs and ephrins in the inner ear (Bianchi and Gale, 1998; Zhou et al., 2011), a role for fasciculation and/or radial bundle formation has not been described.

RESULTS

Pou3f4 is expressed by otic mesenchyme cells during all stages of SGN development

Pou3f4 expression in the otic mesenchyme has been described previously (Ahn et al., 2009; Phippard et al., 1998), but those studies did not determine whether other cells nearby, such as SGNs or associated glia were also positive for Pou3f4. Thus, we conducted a comprehensive temporal/spatial analysis of Pou3f4 protein expression during SGN development using a Pou3f4-specific antibody, along with markers of mature auditory neurons (Tuj1) and Schwann cells (Sox10; Puligilla et al., 2010). In mouse, SGNs develop within the cochleovestibular ganglion (cvg), a transient structure formed by neuroblasts that delaminate from the ventral-medial side of the otocyst at E9.5 (Figure 1A and 1B). At E9.5, Pou3f4 expression in the presumptive mesenchyme is not detectable (Figure 1A), however, at E10.5, small patches of Pou3f4-expressing mesenchyme cells emerge adjacent to the cvg (Figures 1B; see arrows). By E12.5, when the auditory and vestibular components of the

inner ear have diverged (Koundakjian et al., 2007), Pou3f4 is detectable in all compartments of the otic mesenchyme (Figure 1C). At this stage, neural crest-derived Schwann cells infiltrate the ganglia, and SGNs begin to project peripheral axons toward the prosensory domain located within the cochlear epithelium (Carney and Silver, 1983). At these early stages, Pou3f4 is detectable in otic mesenchyme cells, but not in neurons, glia, or epithelia. Moreover, Pou3f4-expressing mesenchyme cells appear to make direct contact with the distal ends of the SGN peripheral axons (Figure 1C; arrowheads) in regions where Schwann cells have not yet arrived. At E16.5, SGN peripheral axon outgrowth continues along the length of the cochlea as the otic mesenchyme (om) population expands to form the future osseous spiral lamina and spiral limbus (osl and sl, respectively; Figure 1D, E). The adult osl consists of bony plates that surround the SGN axons and the sl is a thickened periosteum. At E15.5–E16.5, radial bundles form concurrently with the appearance of bands of mesenchyme cells located between SGN peripheral axons (as in Figure 2G; asterisks). By P2, Pou3f4-positive mesenchyme cells segregate from extending SGN axons, with clearly visible boundaries (Figure 1E). Occasional Pou3f4-positive cells were observed within the somal layer of the spiral ganglion (Figure 1E), but these cells were not positive for either Tuj1 or Sox10, suggesting they are mesenchyme cells that have interspersed the ganglion during development (arrows in Figures 1E,F). In whole-mount at E17.5, the segregation of the peripheral axons and the otic mesenchyme is dramatic: groups of ~50–100 axons fasciculate to form relatively evenly spaced “inner radial bundles” along the length of the cochlea (Figure 1G–I). Higher magnification images show how axons travel in areas that are devoid of Pou3f4 and rarely cross between bundles (Figures 1J–O).

Radial bundle fasciculation is lost in *Pou3f4*$^{y/-}$ embryos

Previously, *Pou3f4* mutants were shown to have variable levels of hypoplasia of the otic mesenchyme and severe hearing impairment (Minowa et al., 1999; Phippard et al., 1999). Therefore, we hypothesized that, if SGN fasciculation and otic mesenchyme organization are interdependent, then inner radial bundle formation may require *Pou3f4*. To test this hypothesis, we compared radial bundle development in whole-mount preparations of *Pou3f4*$^{y/+}$ and *Pou3f4*$^{y/-}$ cochleae (Figure 2A–H). At E17.5, *Pou3f4*$^{y/+}$ cochleae contained dense, well-organized, fascicles that projected directly from the SGN soma to the cochlear epithelium (Figure 2A–C). This pattern is most conspicuous at the base of the cochlea (Figure 2A and 2B), but is also evident at the apex (Figure 2C) where the bundles are always less compact. In contrast, SGN axons in *Pou3f4*$^{y/-}$ embryos failed to fasciculate properly, formed loosely compacted bundles, and contained increased numbers of laterally projecting processes (Figure 2D–F). Although this fasciculation phenotype could arise from a deficit of auditory glia (Breuskin et al., 2010), there appeared to be no defect in their development (Figure 2E; Sox10 staining). Fasciculation defects were evident in *Pou3f4*$^{y/-}$ embryos as early as E15.5 (Figure 2G,H), suggesting disruptions during the early phases of axon outgrowth.

To quantify fasciculation along the length of the cochlea, the total area occupied by SGN axons between the soma and the sensory epithelium was measured (see Experimental Procedures; Figure 2I and J). In base, middle and apical regions of the cochlea, the SGN axons in *Pou3f4*$^{y/-}$ embryos consumed significantly more space compared to their wild type littermates (Figure 2K), with the greatest difference in fasciculation present at the apex (80% vs. 91% respectively; see Figure 2K, light grey bars). In addition, the frequency with which processes crossed between fascicles was significantly greater in *Pou3f4*$^{y/-}$ embryos compared to wild type (Figure 2L; arrows in 2D). *Pou3f4*$^{y/-}$ cochleae have been reported to be slightly shorter than controls, which raised the possibility that the SGN fasciculation defects might result from changes in neuron numbers along the length of the cochlea.

However, a comparison of the density of SGN cell bodies between *Pou3f4*$^{y/+}$ and *Pou3f4*$^{y/-}$ cochleae indicated no significant differences (Figure 2M and Figure S1).

To determine if a loss of surrounding otic mesenchyme cells caused the SGN fasciculation defects in *Pou3f4*$^{y/-}$ mice, we compared the frequency of apoptotic cells in the otic mesenchyme between *Pou3f4*$^{y/+}$ and *Pou3f4*$^{y/-}$ animals using antibodies against cleaved caspase-3 (CC3) (Figure S1E–J). We also used DAPI to look for potential necrotic lesions (Figure S1L–O). Although the density of the mesenchyme cells appeared to be slightly lower in *Pou3f4*$^{y/-}$ animals (Figure S1G and S1J; compare the outlined areas), there was no enhanced apoptosis or necrosis in the otic mesenchyme cells (Figure S1K–S1O).

Innervation and ribbon synapse formation are diminished in *Pou3f4*$^{y/-}$ embryos

Axon fasciculation reduces pathfinding errors and provides efficient innervation of target tissues (Tessier-Lavigne and Goodman, 1996). Considering the fasciculation defects in the *Pou3f4*$^{y/-}$ cochleae, possible changes in innervation were examined. SGNs are subdivided into two classes: types I SGNs (90% of the entire population) which form synapses on inner hair cells, and type II SGNs (the remaining 10%), which grow past the inner hair cell layer, cross the tunnel of Corti, and then turn toward the base before forming synapses with outer hair cells (Huang et al., 2007; Koundakjian et al., 2007). At the base of wild type cochleae at E17.5, Tuj-limmunolabeling shows the dense layer of type I SGN endings, as well as type II processes that cross the pillar cell layer before turning toward the base (Figure 3A). These preparations were counterstained with Sox10 antibodies to reveal the morphology of the cochlear epithelium with respect to the SGNs (Figure 3B, C). Images acquired at the mid-base, mid-apex, and apex (Figure 2D–F) illustrate the base-to-apex maturation of the type II processes. By comparison with *Pou3f4*$^{y/+}$ embryos, *Pou3f4*$^{y/-}$ embryos at E17.5 showed diminished innervation by both types of SGNs: the type I layer of *Pou3f4*$^{y/-}$ embryos was narrowed and less robust (see brackets; Figure 3G–L), and the number of type II processes was substantially reduced (Figure 3G–L). In addition, the type II processes that were present appeared to be shorter and less mature (Figure 3J, K), or non-existent (Figure 3L). Sox10 immunostaining indicated no changes in the morphology of the supporting cells in *Pou3f4*$^{y/-}$ cochleae (Figure 3H, I). These data suggest that fasciculation defects result in diminished target innervation within the cochlear epithelium.

We therefore reasoned that synapse numbers between SGNs and hair cells would also be reduced in *Pou3f4*$^{y/-}$ mice. ~500 nm ribbon-type synapses can be visualized in hair cells and quantified using anti-Ribeye antibodies (Meyer et al., 2009; Fig. 3M–P). Post-synaptic glutamate receptor immunoreactivity has a diffuse appearance at early postnatal stages, but is suitable for qualitative observations (Nemzou et al., 2006; Figure 3M–P). Comparisons at postnatal day eight (P8) indicated fewer ribbon synapses and lower levels of glutamate receptor immunoreactivity in *Pou3f4*$^{y/-}$ mice (Figure 3M–P). Cross-sections of cochleae at P8, immunostained with neurofilament and Ribeye antibodies, confirmed a decrease in the density of type I SGN endings and showed a quantifiable decrease in the number of ribbon synapses (Figure 3Q–X). Consistent with the gradient in innervation defects, the decrease in ribbon synapses was also graded with a mild effect in the base of the cochlea and a more severe effect at the apex (reduced by approximately 30%). These data suggest that disrupting fasciculation impairs the ability of SGNs to locate their targets and form synapses.

Expression of EphA4 is reduced in otic mesenchyme lacking *Pou3f4*

Fasciculation is typically mediated by cell-surface or secreted factors (Tessier-Lavigne and Goodman, 1996), therefore we hypothesized that otic mesenchyme cells from *Pou3f4*$^{y/-}$ mice might fail to express one or multiple factor(s) that directly promote SGN fasciculation.

Microarray results (see Experimental Procedures) comparing mRNAs from *Pou3f4*$^{y/+}$ and *Pou3f4*$^{y/-}$ mesenchyme showed a significant loss of *Epha4*. EphA4 is one of 15 different Eph receptors that interact at the cell-cell interface with nine possible cell surface-bound ephrin ligands to serve diverse developmental functions including axon repulsion/attraction (Eberhart et al., 2002; Kullander and Klein, 2002), cooperative axon targeting (Gallarda et al., 2008), and axon fasciculation (Bossing and Brand, 2002; Orioli et al., 1996). Therefore, the developmental expression pattern of EphA4 in the cochlea was examined (Figure 4A–F). Using *in situ* hybridization, we found that *Epha4* mRNA is broadly distributed at E14.5 (not shown) and E16.5 (Figure 4A and B), localizing to mesenchyme, the spiral ganglion, and the cochlear epithelium. However, we saw a remarkably limited pattern of expression with antibodies specific to the extracellular domain of EphA4 protein: virtually all immunoreactivity was observed in otic mesenchyme cells (Figures 4C–F). A high magnification view of the SGN peripheral axons (Figure 4G and H) shows that EphA4 protein is expressed only by the adjacent mesenchyme cells in a “guide rails” fashion (see *, Figure 4G and H), but is not detectable in the SGN axons (arrowheads) themselves. Importantly, whole-mount preparations and orthogonal reconstructions of E18.5 cochleae show that EphA4 is distributed in the Pou3f4-positive mesenchyme bands between the SGN fascicles, but does not overlap with Tuj1 (Figure 4I–N). These results indicate that EphA4 protein is distributed in a spatial and temporal manner consistent with a role in SGN fasciculation. It is unclear why there is a discrepancy between EphA4 mRNA and protein distribution, but a post-transcriptional regulatory program that limits EphA4 protein to the mesenchyme may be present.

To confirm that EphA4 expression in the mesenchyme depends on *Pou3f4*, we used quantitative PCR to show an approximate five-fold reduction in *Epha4* expression in *Pou3f4*$^{y/-}$ cochleae (Figure 4O). Moreover, analyses of whole-mount preparations from *Pou3f4*$^{y/-}$ cochleae show that EphA4 protein is substantially reduced in the otic mesenchyme at E17.5 (Figure 4P–U).

EphA4 promotes SGN fasciculation and hair cell innervation

If Pou3f4 transcriptional activity regulates *Epha4* expression in the otic mesenchyme to promote SGN fasciculation, we reasoned that *Epha4*-deficient mice should also have fasciculation defects. We therefore examined the SGNs from *Epha4*$^{-/-}$ embryos at late embryonic ages (Helmbacher et al., 2000; North et al., 2009). Compared to their wild-type littermates (Figure 5A, C, E, G), *Epha4*$^{-/-}$ mice presented fasciculation defects that were remarkably similar to those observed in the *Pou3f4*$^{y/-}$ animals (Figure 5B, D, F, H; compare to Fig. 2). Whereas wild-type cochleae showed tight SGN bundles and well-defined mesenchyme bands (Figure 5A,C), the SGNs in *Epha4*$^{-/-}$ cochleae displayed dispersed, poorly fasciculated bundles that aberrantly traversed the mesenchymal space (Figure 5B,D), and occupied significantly more area at the basal, mid-modiolar, and apical regions of the cochlea (Figure 5I). Orthogonal reconstructions of these samples illustrate disruptions in the normal interdigitation of the mesenchyme cells and the SGN bundles in the *Epha4*$^{-/-}$ mutants (Figure 5E,F). The number of mesenchyme cells in *Epha4*$^{-/-}$ cochleae appeared unchanged compared to wild type, suggesting that the fasciculation defects in the SGNs are not due to a loss of surrounding mesenchyme (Figure 5G, H). Similar to SGNs from *Pou3f4*$^{y/-}$ mice, SGNs from *Epha4*$^{-/-}$ mice showed an approximately four-fold increase in the number of axons that crossed between bundles (Figure 5J). Finally, we examined *Epha4*$^{-/-}$ cochleae at P7 to determine if these animals (like *Pou3f4*$^{y/-}$ mice) had defects in hair cell innervation and ribbon synapse formation (Figure S2). Due to early postnatal lethality of this line, we were only able to examine four mutant ears, thus our conclusions are based on a limited sampling. Compared to controls (S3A, C and D), *Epha4*$^{-/-}$ mice showed a nearly two-fold reduction in the number of ribbon synapses (Figure S2B, E and F),

further supporting that SGN fasciculation is important for target innervation. Overall, the fasciculation and synapse defects in *Epha4* and *Pou3f4* mutants are very similar, consistent with their participation in a common developmental process.

To investigate whether EphA4 plays a non-cell autonomous role during SGN fasciculation, we asked whether exogenous EphA4 extracellular domains (serving as a substitute for mesenchyme) could promote SGN fasciculation *in vitro*. E12.5 spiral ganglia were cultured for 24 h (without otic mesenchyme) on a layer of Matrigel infused with either control Fc or EphA4-Fc (Figure 5K–M), to determine the effects on fasciculation. We also examined the effects of preclustering EphA4-Fc to determine whether “activating” (preclustered form) or “blocking” (unclustered form) ephrin ligands on the SGNs had different effects on fasciculation (Davis et al., 1994). In the presence of control Fc (preclustered), SGN explants projected mostly single neurites and some rudimentary fascicles (Figure 5K, see arrows), suggesting that SGNs may have some intrinsic axo-axonal binding capacity. However, explants cultured with preclustered EphA4-Fc showed dramatically enhanced fasciculation, with thick bundles projecting away from the soma (Figure 5L) and very few single neurites. Interestingly, EphA4-Fc treatments did not reduce the length of axons (growth cone collapse) compared to controls (not shown). When we stained these cultures with anti-Integrin-α6 antibodies to mark the auditory glia, we found their growth pattern to be almost identical to that of the SGNs, raising the possibility that the glia may also respond to EphA4. However, when the SGNs were eliminated in the presence of high pH culture medium (Mukai et al., 2011), but grown in preclustered EphA4-Fc, the glia persisted, but did not bundle (Figure 5M), suggesting that SGN fasciculation is not normally a secondary response to aggregating glia. Preclustered EphA4-Fc at 10 nM led to a 4-fold increase in average bundle diameter compared to controls (Figure 5N), and doubled the percentage of fascicles greater than 3.5 μm in diameter (Figure 5O). Importantly, cultures grown in the presence of unclustered EphA4-Fc showed levels of bundling that were not significantly different from controls (see Figure 5N and O), suggesting that blocking ephrins from recognizing Eph receptors on neighboring axons or glia has little effect on SGN fasciculation. These results demonstrate that EphA4, expressed by mesenchyme cells, may normally activate ephrin ligands expressed by SGNs to promote fasciculation.

Pou3f4 knockdown *in vitro* causes SGN fasciculation defects that are rescued by EphA4

To determine if Pou3f4 and EphA4 are functionally linked, we established an *in vitro* system to investigate SGN fasciculation using explanted SGNs and otic mesenchyme. At E12.5, the auditory component of the cochleo-vestibular ganglion can be easily isolated and co-cultured with pieces of otic mesenchyme; over time these cell populations intercalate, while developing SGNs extend processes (Figure 6A; Figure S3). In these assays, the SGNs appear to briefly migrate away from the explant, and then extend axons (often in clusters with other neurons; see Figure S3), at the same time mesenchyme cells invade. In addition, co-culturing the SGNs and mesenchyme in a thick Matrigel layer allows the two cell populations to interact in a semi-three dimensional gel, mimicking SGN fasciculation *in vivo* (Figure S3B and C). To examine the effects of decreased expression of Pou3f4, Morpholino antisense oligonucleotides (MOs) were used to knock-down Pou3f4. Figure 6A shows uptake of a control MO- fluorescein isothiocyanate (FITC) conjugate by endocytic vesicles in mesenchyme and neurons. A Pou3f4-specific antisense MO at 20 μM showed a nearly complete knockdown of Pou3f4 (Figure 6B). Treatment with the Pou3f4 MO also induced a significant knockdown of *Epha4* (Figure 6C), confirming a direct effect for Pou3f4 on *Epha4* expression.

The soma of SGNs maintained in co-culture with control MO were typically clustered with one another (Fig 6D,E) and their neurites often formed extensive and straight fascicles that extended through the mesenchyme cells (Figure 6F; Figure S3)(Simmons et al., 2011). By

contrast, when cultures were treated with the Pou3f4 MO, SGNs failed to form clusters (Figure 6G,H). Distal processes still extended amongst the otic mesenchyme cells, but these processes failed to fasciculate and often followed more torturous paths (Figure 6I), similar to *Pou3f4*$^{y/-}$ cochleae. To quantify these effects, average SGN fascicle diameter was determined for both conditions. In controls, average fascicle diameter was approximately 3.1 μm (Figure 6K; individual SGN neurites in culture are small, typically ~1 μm in diameter) and 28% of fascicles were classified as "large" fascicles (larger than or equal to 3.5 μm; Figure 6L). Fascicles in Pou3f4 MO-treated cultures had a significantly smaller average diameter of 2 μm and only eight percent of the fascicles were classified as "large" (Figure 6L). To determine whether fasciculation loss was a result of down-regulating EphA4, EphA4-Fc protein was added to SGN/mesenchyme cultures that had been treated with the *Pou3f4* MO. The addition of preclustered EphA4-Fc restored SGN fasciculation (Figure 6J) and induced a statistically significant increase in fascicle diameter size, as well as a 12% enhancement of "large" fascicles (Figure 6K,L).

Ephrin-B2 acts as a cofactor for EphA4 during SGN fasciculation

We next reasoned that, if EphA4 expression by otic mesenchyme cells promotes SGN fasciculation, then at least one ephrin cofactor must be expressed by the SGNs. Thus, an extensive *in situ* hybridization survey was performed to determine which of the 7 known EphA4 ligands (Wilkinson, 2001) are expressed by SGNs during mid-to-late gestation (Figure S4; Figure 7). For *Efna1*, *Efna5*, and, *Efnb3*, mRNA was not detectable at appreciable levels in the cochlea (not shown). Transcripts for both *Efnb2* and *Efna4* were distributed broadly in the cochlea, including the spiral ganglion, and *Efna3* appeared in the SGNs, but at a level just slightly above the control probe (Figure S4). In contrast, *Efnb2* was detected at high levels in SGNs at E13.5 (Figure 7A), and E15.5 when SGN fasciculation commences (Figure 7B and C). Ephrin-B2 protein was similarly detected in the SGNs and their axons by immunostaining (Figure 7D), and overlapped primarily with neuronal markers (Tuj1; Figure 7E, F and H; see arrows), but not with markers of auditory glia (Integrin-α6; Figure7G and H; see arrowheads). The complementary expression of ephrin-B2 on SGN axons and EphA4 on adjacent mesenchyme (compare Figure 7D to 4F) suggested that ephrin-B2 is spatially and temporally positioned to interact with EphA4 during SGN fasciculation.

We next predicted that, if EphA4 signals through ephrin-B2 in this system, then blocking ephrin-B2 function using unclustered ephrin-B2-Fc would prevent SGN fasciculation in SGN/mesenchyme co-cultures similar to the effects of the Pou3f4 MO. Consistent with this hypothesis, ephrin-B2-Fc led to a nearly 25% decrease in fascicle diameter, and a more-than 4-fold decrease in the number of "large fascicles" as compared to control (Figure 7I–L). We next asked whether the loss of *Efnb2* in the SGNs *in vivo* would lead to fasciculation defects similar to those observed in the *Pou3f4* and *Epha4* mutants. Because *Efnb2* was detectable in regions of the cochlea besides the SGNs, particularly at earlier stages (Figure 7A, B, and D), we conditionally removed *Efnb2* in the SGNs by crossing *Efnb2 loxP* mice (Gerety and Anderson, 2002) to mice carrying *Ngn-CreERT2* (Koundakjian et al., 2007), a transgene that shows robust reporter activity in the SGNs after tamoxifen delivery (Figure 7M). Resulting *Efnb2* conditional knock out (cko) mice showed substantially reduced levels of ephrin-B2 protein, particularly in the SGN peripheral axons (Figure S4), but not in other regions of the cochlea.

Compared to Cre-positive wild-type littermate controls (Figures 7N and P), the SGNs from *Efnb2 cko* cochleae showed both fasciculation defects and axons that aberrantly crossed between fascicles, but did not show a loss of mesenchyme (Figure 7O and Q). Although statistically significant in some cases, these defects were less severe compared to what we observed in the *Pou3f4* or *Epha4* mutants, likely owing to functional redundancy by other

ephrins present, or possibly a lack of complete ephrin-B2 elimination. *Efnb2* cko cochleae showed a 6% increase in area consumed by axons and maximally a 4-fold increase in the number of axons that crossed between bundles (Figures 7R and S). Because tamoxifen was given at a single does at E9.5–E10.5, most defects were observed at the base and mid-modiolar regions of the cochlea, in accordance with previous studies with *Ngn-CreERT2* (Koundakjian et al., 2007). Importantly, the *Efnb2 cko* phenotype was similar to the fasciculation phenotypes observed in both the *Pou3f4* and *Epha4* mutants lines, suggesting that ephrin-B2 may function as a ligand for EphA4 in this process.

Pou3f4 associates with *EphA4* regulatory elements

We next asked whether, in the developing otic mesenchyme, regulatory elements of *Epha4* are a direct target of Pou3f4. Pou proteins are known to have a bipartite DNA binding system that includes a POU-specific domain, as well as a homeobox domain (Phillips and Luisi, 2000). Whereas the recognition sequences of several Pou proteins have been characterized, relatively little is known about mouse Pou3f4. However, one report has demonstrated that Pou3f4 preferentially recognizes the tandem homeobox sequence ATTATTA in the regulation of the Dopamine Receptor 1A gene *D1A* (Okazawa et al., 1996). Therefore, we scanned the entire *Epha4* genomic sequence and found four of these sites within introns in the first 70 kilobases (kb), and one approximately 8.5 kb upstream of exon one (Figure 8A). We then performed chromatin immunoprecipitation (ChIP) using otic mesenchyme and a Pou3f4-specific IgY, and assayed the resulting DNAs for these *Epha4* regulatory regions using quantitative PCR (Figure 8B). In these experiments β-*actin*, *Neurogenin-1*, and an *Epha4* site that did not contain ATTATTA, were used as negative controls; there was no significant association at these sites with the control or Pou3f4-specific IgY. However, all five of the putative *Epha4* regulatory regions showed preferential association (with statistical significance) with the Pou3f4-specific IgY with little to no association with the control IgY (Figure 8B). These data suggest that Pou3f4 may directly regulate *Epha4* in otic mesenchyme cells in order to initiate EphA4-mediated SGN fasciculation.

DISCUSSION

The results presented in this study reveal a new and intriguing role for otic mesenchyme in the development of cochlear innervation. Moreover, the identification of additional auditory defects arising from the absence of *Pou3f4* provides insights into the underlying basis for the deafness that occurs in both human and murine mutants. Previous reports have demonstrated a significant decrease in endocochlear potential that is almost certainly a major component of the auditory dysfunction, but the demonstration of a 30% decrease in the number of ribbon synapses may indicate a significant loss in acuity. While this hypothesis cannot be tested without a mouse model in which endocochlear potential is preserved, it would need to be considered in terms of developing any potential therapeutic interventions.

The results presented here identify a novel molecular signaling pathway in which Pou3f4 expression in otic mesenchyme cells directly activates *Epha4*, leading to the expression of EphA4 on the surface of these cells (Figure 8C). The presence of EphA4 provides a cue that acts, along with the spatial distribution of otic mesenchyme, to promote fasciculation of SGNs via binding to ephrin-B2 on their surfaces. Furthermore, these data predict that EphA4 activates ephrin-B2 to generate a reverse signaling response to segregate the SGNs and mesenchyme in a manner classically documented in zebrafish animal cap assays (Mellitzer et al., 1999). However, the mechanism(s) by which ephrin-B2 promotes fasciculation among the SGN axons remains unclear. Ephrin-B2 reverse signaling may induce filopodial collapse (Cowan and Henkemeyer, 2001) by the SGN growth cones, which, by default, may lead them to preferentially associate with neighboring axons. Or, ephrin-B2 reverse signaling

may promote SGN interaxonal adhesion by signaling to other cell-surface factors known to regulate fasciculation, such as IgCAMs (Lin et al., 1994) and/or integrins (Baum and Garriga, 1997).

These results reveal the molecular basis for the organizing effects of otic mesenchyme as well as the first demonstration of a paracrine mode of action for Pou3f4 in axon guidance. Interestingly, Pou4F2 (Brn3b) is known to regulate axon pathfinding and fasciculation in retinal ganglion cells through an autocrine signaling pathway (Pan et al., 2008), and in *Drosophila*, deletion of the *Pou3f4* ortholog *ventral veins lacking* (*vvl*), leads to defects in fasciculation and steering of axons in the fly brain, although much of these defects may be secondary to effects on neuronal specification (Meier et al., 2006). In addition, while this is the first demonstration of a role for Eph-ephrin signaling in the initial development of the peripheral auditory system, elegant work by Cramer et al., has already demonstrated a role for EphA4 in hearing and central auditory plasticity. These authors showed that, after surgically removing the cochlea (and peripheral input to the brain), the expression of *Epha4* was critical for target selection during remodeling (Hsieh et al., 2007; Miko et al., 2008). The functions of ephrin-Eph receptor interactions likely go well beyond those presented here and in previous publications. As shown in Figure S4 and in previous reports, several other ephrins and Ephs are expressed in the cochlea (Bianchi and Gale, 1998; Zhou et al., 2011) and may serve a variety additional functions. This may also indicate why EphA4-Fc was only able to partially rescue the fasciculation defects in the absence of Pou3f4 (Figure 6). In particular, axon-axon interactions by Ephs and ephrins may also play a role in SGN radial bundle formation, similar to the coordinated actions of motor and sensory axons, as has been shown recently (Gallarda et al., 2008; Wang et al., 2011). Indeed, when cultured in the absence of mesenchyme, SGNs have some intrinsic capacity to fasciculate. Inhibiting ephrins expressed on SGNs with unclustered EphA4-Fc did not diminish fasciculation compared to controls (Figure 5), but a more complete characterization of other Eph-ephrin interactions would be required to eliminate this possibility.

The innervation patterns of the mammalian auditory system are remarkably complex, containing multiple fiber and bundle types (reviewed in Appler and Goodrich, 2011). Despite a wealth of descriptive and functional studies beginning as early as the late-1800s, the specific functions of different fiber tracts and neuronal cell types are only now being elucidated. Mutations in *Pou3f4, Epha4* or *Efnb2* lead to defects in the formation of radial fiber bundles, but the functions of these bundles are unknown. Considering their regular alignment along the tonotopic axis of the cochlea, it has been suggested these each bundle may contain fibers tuned to a specific frequency and that radial bundle formation may thus play an important role coordinating frequency matching between SGNs and auditory hair cells (Rubel and Fritzsch, 2002). If this is the case, then defects in radial bundle formation, such as those reported in this study, could lead to significant tonotopic defects in the cochlea and possibly higher CNS auditory nuclei. This conclusion is supported by the significant functional and morphological defects in the auditory systems of *Epha4* and *Efnb2* mutant mice (Miko et al., 2008) with ABR waveform signatures suggesting defects both peripherally and centrally. Unfortunately, the direct roles of EphA4 and ephrin-B2 in the formation of tonotopic organization in the auditory brainstem make it impossible to discern the specific effects of defects in radial bundle formation without generating inner ear specific mutants.

The increased number of crossing fibers and the decrease in ribbon synapses observed in *Pou3f4/Epha4/Efnb2* mutants indicate that fasciculation signals arising from surrounding otic mesenchyme clearly act to prevent routing errors within the mesenchymal space by driving SGN fibers onto existing radial bundles. Previous studies indicated that otic mesenchyme cells express EphA4 protein (Pickles et al., 2002; van Heumen et al., 2000),

and that EphA4 prevented outgrowth of mature SGNs in vitro (Brors et al., 2003). However, the results presented here demonstrate that for immature SGNs, rather than inhibiting axon outgrowth, EphA4/ephrin-B2 interactions act to form a barrier that promotes SGN fasciculation without affecting outgrowth. Overall, the factors that guide SGN axons during their pathfinding remain unknown. Neurotrophin signaling through TrkB and TrkC, while critical for growth and maintenance of SGNs, is not required for the directed outgrowth of SGNs (Fekete and Campero, 2007; Fritzsch et al., 2005). Additional studies will clearly be required to identify the neurotropic factors for SGNs.

EXPERIMENTAL PROCEDURES

Animal care and tissue preparation

All animals used in this study were maintained in accordance with the NIH Care and Use Committee. Timed pregnant CD1 mice (Charles River Laboratories) were used for protein expression studies and neuron/mesenchyme explant cultures. *Pou3f4* mutant mice, in which the coding region was replaced with Cre recombinase, were maintained on a mixed background. This line phenocopies a previously published *Pou3f4* knockout mouse (Phippard et al., 1999). Because *Pou3f4* is on the X-chromosome, only males were used in this study in order to avoid variability arising from X-inactivation. In order to generate hemizygous males, $Pou3f4^{+/-}$ females were crossed to wild-type CD1 males. To generate conditional *Efnb2* knockout animals (*Efnb2* cko), C57/BL6 *Efnb2 flox/flox* mice (Gerety and Anderson, 2002) were bred with mice carrying the *Neurogenin (Ngn)-CreERT2* transgene (Koundakjian et al., 2007) on a mixed CD1 background. $Ngn1^{CreERT2}$; $Efnb2^{flox/+}$ mice were crossed, and pregnant dams were gavaged with a single dose of tamoxifen (Sigma; solubilized in flax and sunflower seed oil; 0.5 mg/40 g body weight) at 9.5–10.5 days gestation. Using this strategy, we found Cre reporter activity in 95–100% of SGNs at the cochlear base (R26R-YFP; Jackson Laboratory; Figure 7).

Immunostaining and *in situ* hybridization

For whole-mount immunostaining of the SGN, cochleae were isolated from the vestibular components, bony capsule, and associated stria. Following permeabilization with 0.5% Triton X-100 and blocking with 10% serum, the cochleae were incubated overnight at 4°C in primary antibodies, and then rinsed extensively. Fluorescent secondary antibodies (Invitrogen, 1:1000) were applied for 1h at room temperature. For culture explants and cryoprotected tissue sections, antibody staining was performed as described previously (Driver et al., 2008). Confocal z-stack images were obtained using an LSM-510 (Zeiss), projected using NIH-ImageJ, and then further processed using Adobe Photoshop. *In situ* hybridization was performed as described (Raft et al., 2007). For all templates, sense controls were generated in parallel. Tissue processing, sectioning, hybridization and detection were performed as previously described (Raft et al., 2007).

Neuron and mesenchyme culture experiments

CD1 embryos were prepared for culture experiments as described previously (Montcouquiol et al., 2003). Culture medium included DMEM, 10% fetal bovine serum, 0.2% N2, and . 001% Ciprofloxacin. In pilot experiments, we determined that the spiral ganglion persisted in culture up to 5 days without additional neurotrophins only if the glia were not removed. For the 24 h Matrigel outgrowth assays, MatTek dishes (MatTek corporation) were coated (24 hours at 37°C) with 10% Matrigel mixed with either human IgG-Fc (Jackson Immunoresearch) or EphA4-Fc (R&D Systems). To pre-cluster the Fc fusion proteins for some experiments, each Fc protein was combined with mouse-anti-human Fc (Jackson Immunoresearch) for 1 hour at a 1:10 molar ratio. For each experiment, the spiral ganglion

was removed at E12.5 and placed onto a pre-coated dish with normal culture medium and permitted to grow for 24 h.

For neuron/mesenchyme co-culture experiments, a spiral ganglion and an equivalentsized portion of otic mesenchyme were removed from the cochlea at E12.5 and transferred to Matrigel-coated MatTek dishes (5% for 1 h at 37°C), containing solutions of either standard control MO or a Pou3f4-specific MO (GATCCTCTACTAGTTATAATGTGGC). Neuron and mesenchyme explants were plated approximately 1 mm from each other before receiving Endoporter (0.6% final; Gene-Tools) to facilitate delivery of the MOs. After 2d at 37°C, the MO/Endoporter-containing medium was replaced with normal culture medium, and grown an additional 3d. For some experiments, soluble pre-clustered human IgG-Fc or EphA4-Fc, were added to cultures following 2d Morpholino exposure. Both IgG-Fc and EphA4-Fc were used at 10 nM based on a previous report (Brors et al., 2003). For culture experiments comparing Fc vs. ephrin-B2-Fc (R&D Systems), preclustering was not performed.

Chromatin Immunoprecipitation (ChIP)

ChIP was performed as described previously (Jhingory et al., 2010), but with minor modification. E15.5 cochleae were isolated in chilled PBS and then fixed for 20 minutes using 4% paraformaldehyde. The Agarose ChIP Kit (Pierce) was used for subsequent DNA digestion and precipitation. Approximately 8 μg of chicken-anti-Pou3f4 or chicken IgY (negative control) and PrecipHen beads (Aves Labs) were used for IP. With resulting DNAs, qPCR using SYBR Green was performed. For each primer set, a standard curve was generated using mouse genomic DNA; control and experimental C_t values were compared to this standard curve for quantification. The data here represents at least two independent ChIPs and three qPCR analyses for each primer set.

Supplementary Material

Refer to Web version on PubMed Central for supplementary material.

Acknowledgments

We thank the members of the Kelley lab for their valuable discussions and technical assistance during this work. We thank Drs. Lisa Cunningham (NIH/NIDCD), Doris Wu (NIH/NIDCD), and Maria J. Donoghue (Georgetown University) for the critical reading of this manuscript. *Epha4* null tissue was a kind gift from M.J. Donoghue. Mr. Jonathan Stuckey was very helpful with the illustration in Figure 8. The National Deafness and Other Communication Disorders Intramural Research Program funded this work.

REFERENCES

Ahn KJ, Passero F Jr. Crenshaw EB 3rd. Otic mesenchyme expression of Cre recombinase directed by the inner ear enhancer of the Brn4/Pou3f4 gene. Genesis. 2009; 47:137–141. [PubMed: 19217071]

Appler JM, Goodrich LV. Connecting the ear to the brain: Molecular mechanisms of auditory circuit assembly. Prog Neurobiol. 2011

Baum PD, Garriga G. Neuronal migrations and axon fasciculation are disrupted in ina-1 integrin mutants. Neuron. 1997; 19:51–62. [PubMed: 9247263]

Bianchi LM, Gale NW. Distribution of Eph-related molecules in the developing and mature cochlea. Hear Res. 1998; 117:161–172. [PubMed: 9557986]

Bossing T, Brand AH. Dephrin, a transmembrane ephrin with a unique structure, prevents interneuronal axons from exiting the Drosophila embryonic CNS. Development. 2002; 129:4205–4218. [PubMed: 12183373]

Breuskin I, Bodson M, Thelen N, Thiry M, Borgs L, Nguyen L, Stolt C, Wegner M, Lefebvre PP, Malgrange B. Glial but not neuronal development in the cochleovestibular ganglion requires Sox10. J Neurochem. 2010; 114:1827–1839. [PubMed: 20626560]

Brors D, Bodmer D, Pak K, Aletsee C, Schafers M, Dazert S, Ryan AF. EphA4 provides repulsive signals to developing cochlear ganglion neurites mediated through ephrin-B2 and -B3. J Comp Neurol. 2003; 462:90–100. [PubMed: 12761826]

Carney PR, Silver J. Studies on cell migration and axon guidance in the developing distal auditory system of the mouse. J Comp Neurol. 1983; 215:359–369. [PubMed: 6863589]

Coate TM, Swanson TL, Copenhaver PF. Reverse signaling by glycosylphosphatidylinositol-linked Manduca ephrin requires a SRC family kinase to restrict neuronal migration in vivo. J Neurosci. 2009; 29:3404–3418. [PubMed: 19295147]

Cowan CA, Henkemeyer M. The SH2/SH3 adaptor Grb4 transduces B-ephrin reverse signals. Nature. 2001; 413:174–179. [PubMed: 11557983]

Davis S, Gale NW, Aldrich TH, Maisonpierre PC, Lhotak V, Pawson T, Goldfarb M, Yancopoulos GD. Ligands for EPH-related receptor tyrosine kinases that require membrane attachment or clustering for activity. Science. 1994; 266:816–819. [PubMed: 7973638]

Driver EC, Kelley MW. Specification of cell fate in the mammalian cochlea. Birth Defects Res C Embryo Today. 2009; 87:212–221. [PubMed: 19750520]

Driver EC, Pryor SP, Hill P, Turner J, Ruther U, Biesecker LG, Griffith AJ, Kelley MW. Hedgehog signaling regulates sensory cell formation and auditory function in mice and humans. J Neurosci. 2008; 28:7350–7358. [PubMed: 18632939]

Eberhart J, Swartz ME, Koblar SA, Pasquale EB, Krull CE. EphA4 constitutes a population-specific guidance cue for motor neurons. Dev Biol. 2002; 247:89–101. [PubMed: 12074554]

Fekete DM, Campero AM. Axon guidance in the inner ear. Int J Dev Biol. 2007; 51:549–556. [PubMed: 17891716]

Fritzsch B, Pauley S, Matei V, Katz DM, Xiang M, Tessarollo L. Mutant mice reveal the molecular and cellular basis for specific sensory connections to inner ear epithelia and primary nuclei of the brain. Hear Res. 2005; 206:52–63. [PubMed: 16080998]

Gallarda BW, Bonanomi D, Muller D, Brown A, Alaynick WA, Andrews SE, Lemke G, Pfaff SL, Marquardt T. Segregation of axial motor and sensory pathways via heterotypic trans-axonal signaling. Science. 2008; 320:233–236. [PubMed: 18403711]

Gerety SS, Anderson DJ. Cardiovascular ephrinB2 function is essential for embryonic angiogenesis. Development. 2002; 129:1397–1410. [PubMed: 11880349]

Helmbacher F, Schneider-Maunoury S, Topilko P, Tiret L, Charnay P. Targeting of the EphA4 tyrosine kinase receptor affects dorsal/ventral pathfinding of limb motor axons. Development. 2000; 127:3313–3324. [PubMed: 10887087]

Hsieh CY, Hong CT, Cramer KS. Deletion of EphA4 enhances deafferentation-induced ipsilateral sprouting in auditory brainstem projections. J Comp Neurol. 2007; 504:508–518. [PubMed: 17702003]

Huai J, Drescher U. An ephrin-A-dependent signaling pathway controls integrin function and is linked to the tyrosine phosphorylation of a 120-kDa protein. J Biol Chem. 2001; 276:6689–6694. [PubMed: 11053419]

Huang LC, Thorne PR, Housley GD, Montgomery JM. Spatiotemporal definition of neurite outgrowth, refinement and retraction in the developing mouse cochlea. Development. 2007; 134:2925–2933. [PubMed: 17626062]

Jhingory S, Wu CY, Taneyhill LA. Novel insight into the function and regulation of alphaN-catenin by Snail2 during chick neural crest cell migration. Dev Biol. 2010; 344:896–910. [PubMed: 20542025]

Kandpal G, Jacob AN, Kandpal RP. Transcribed sequences encoded in the region involved in contiguous deletion syndrome that comprises X-linked stapes fixation and deafness. Somat Cell Mol Genet. 1996; 22:511–517. [PubMed: 9131020]

Kelley MW. Regulation of cell fate in the sensory epithelia of the inner ear. Nat Rev Neurosci. 2006; 7:837–849. [PubMed: 17053809]

Koundakjian EJ, Appler JL, Goodrich LV. Auditory neurons make stereotyped wiring decisions before maturation of their targets. J Neurosci. 2007; 27:14078–14088. [PubMed: 18094247]

Kullander K, Klein R. Mechanisms and functions of Eph and ephrin signalling. Nat Rev Mol Cell Biol. 2002; 3:475–486. [PubMed: 12094214]

Lin DM, Fetter RD, Kopczynski C, Grenningloh G, Goodman CS. Genetic analysis of Fasciclin II in Drosophila: defasciculation, refasciculation, and altered fasciculation. Neuron. 1994; 13:1055–1069. [PubMed: 7946345]

Meier S, Sprecher SG, Reichert H, Hirth F. ventral veins lacking is required for specification of the tritocerebrum in embryonic brain development of Drosophila. Mech Dev. 2006; 123:76–83. [PubMed: 16326080]

Mellitzer G, Xu Q, Wilkinson DG. Eph receptors and ephrins restrict cell intermingling and communication. Nature. 1999; 400:77–81. [PubMed: 10403252]

Meyer AC, Frank T, Khimich D, Hoch G, Riedel D, Chapochnikov NM, Yarin YM, Harke B, Hell SW, Egner A, Moser T. Tuning of synapse number, structure and function in the cochlea. Nat Neurosci. 2009; 12:444–453. [PubMed: 19270686]

Miko IJ, Henkemeyer M, Cramer KS. Auditory brainstem responses are impaired in EphA4 and ephrin-B2 deficient mice. Hear Res. 2008; 235:39–46. [PubMed: 17967521]

Minowa O, Ikeda K, Sugitani Y, Oshima T, Nakai S, Katori Y, Suzuki M, Furukawa M, Kawase T, Zheng Y. Altered cochlear fibrocytes in a mouse model of DFN3 nonsyndromic deafness. Science. 1999; 285:1408–1411. [PubMed: 10464101]

Montcouquiol M, Rachel RA, Lanford PJ, Copeland NG, Jenkins NA, Kelley MW. Identification of Vangl2 and Scrb1 as planar polarity genes in mammals. Nature. 2003; 423:173–177. [PubMed: 12724779]

Mukai S, Nakagawa H, Ichikawa H, Miyazaki S, Nishimura K, Matsuo S. Effects of extracellular acidic-alkaline stresses on trigeminal ganglion neurons in the mouse embryo in vivo. Arch Toxicol. 2011; 85:149–154. [PubMed: 20480362]

Nemzou NR, Bulankina AV, Khimich D, Giese A, Moser T. Synaptic organization in cochlear inner hair cells deficient for the CaV1.3 (alpha1D) subunit of L-type Ca2+ channels. Neuroscience. 2006; 141:1849–1860. [PubMed: 16828974]

North HA, Zhao X, Kolk SM, Clifford MA, Ziskind DM, Donoghue MJ. Promotion of proliferation in the developing cerebral cortex by EphA4 forward signaling. Development. 2009; 136:2467–2476. [PubMed: 19542359]

Okazawa H, Imafuku I, Minowa MT, Kanazawa I, Hamada H, Mouradian MM. Regulation of striatal D1A dopamine receptor gene transcription by Brn-4. Proc Natl Acad Sci U S A. 1996; 93:11933–11938. [PubMed: 8876240]

Orioli D, Henkemeyer M, Lemke G, Klein R, Pawson T. Sek4 and Nuk receptors cooperate in guidance of commissural axons and in palate formation. EMBO J. 1996; 15:6035–6049. [PubMed: 8947026]

Pan L, Deng M, Xie X, Gan L. ISL1 and BRN3B co-regulate the differentiation of murine retinal ganglion cells. Development. 2008; 135:1981–1990. [PubMed: 18434421]

Pasquale EB. Eph receptor signalling casts a wide net on cell behaviour. Nat Rev Mol Cell Biol. 2005; 6:462–475. [PubMed: 15928710]

Phillips K, Luisi B. The virtuoso of versatility: POU proteins that flex to fit. J Mol Biol. 2000; 302:1023–1039. [PubMed: 11183772]

Phippard D, Heydemann A, Lechner M, Lu L, Lee D, Kyin T, Crenshaw EB 3rd. Changes in the subcellular localization of the Brn4 gene product precede mesenchymal remodeling of the otic capsule. Hear Res. 1998; 120:77–85. [PubMed: 9667433]

Phippard D, Lu L, Lee D, Saunders JC, Crenshaw EB 3rd. Targeted mutagenesis of the POU-domain gene Brn4/Pou3f4 causes developmental defects in the inner ear. J Neurosci. 1999; 19:5980–5989. [PubMed: 10407036]

Pickles JO, Claxton C, Van Heumen WR. Complementary and layered expression of Ephs and ephrins in developing mouse inner ear. J Comp Neurol. 2002; 449:207–216. [PubMed: 12115675]

Puligilla C, Dabdoub A, Brenowitz SD, Kelley MW. Sox2 induces neuronal formation in the developing mammalian cochlea. J Neurosci. 2010; 30:714–722. [PubMed: 20071536]

Puligilla C, Kelley MW. Building the world's best hearing aid; regulation of cell fate in the cochlea. Curr Opin Genet Dev. 2009; 19:368–373. [PubMed: 19604683]

Raft S, Koundakjian EJ, Quinones H, Jayasena CS, Goodrich LV, Johnson JE, Segil N, Groves AK. Cross-regulation of Ngn1 and Math1 coordinates the production of neurons and sensory hair cells during inner ear development. Development. 2007; 134:4405–4415. [PubMed: 18039969]

Rubel EW, Fritzsch B. Auditory system development: primary auditory neurons and their targets. Annu Rev Neurosci. 2002; 25:51–101. [PubMed: 12052904]

Ruben RJ. Development of the inner ear of the mouse: a radioautographic study of terminal mitoses. Acta Otolaryngol. 1967; (Suppl 220):221–244.

Ryan AK, Rosenfeld MG. POU domain family values: flexibility, partnerships, and developmental codes. Genes Dev. 1997; 11:1207–1225. [PubMed: 9171367]

Samadi DS, Saunders JC, Crenshaw EB 3rd. Mutation of the POU-domain gene Brn4/Pou3f4 affects middle-ear sound conduction in the mouse. Hear Res. 2005; 199:11–21. [PubMed: 15574296]

Simmons, D.; Duncan, J.; Crapon de Caprona, D.; Fritzsch, B. Development of the Inner Ear Efferent System/Spring Handbook of Auditory Research. Vol. Vol 38. 2011.

Smith CA. Innervation pattern of the cochlea. The internal hair cell. Trans Am Otol Soc. 1961; 49:35–60. [PubMed: 13914159]

Tessier-Lavigne M, Goodman CS. The molecular biology of axon guidance. Science. 1996; 274:1123–1133. [PubMed: 8895455]

van Heumen WR, Claxton C, Pickles JO. Expression of EphA4 in developing inner ears of the mouse and guinea pig. Hear Res. 2000; 139:42–50. [PubMed: 10601711]

Wang L, Klein R, Zheng B, Marquardt T. Anatomical Coupling of Sensory and Motor Nerve Trajectory via Axon Tracking. Neuron. 2011; 71:263–277. [PubMed: 21791286]

Wilkinson DG. Multiple roles of EPH receptors and ephrins in neural development. Nat Rev Neurosci. 2001; 2:155–164. [PubMed: 11256076]

Zhou CQ, Lee J, Henkemeyer MJ, Lee KH. Disruption of ephrin B/Eph B interaction results in abnormal cochlear innervation patterns. Laryngoscope. 2011; 121:1541–1547. [PubMed: 21647913]

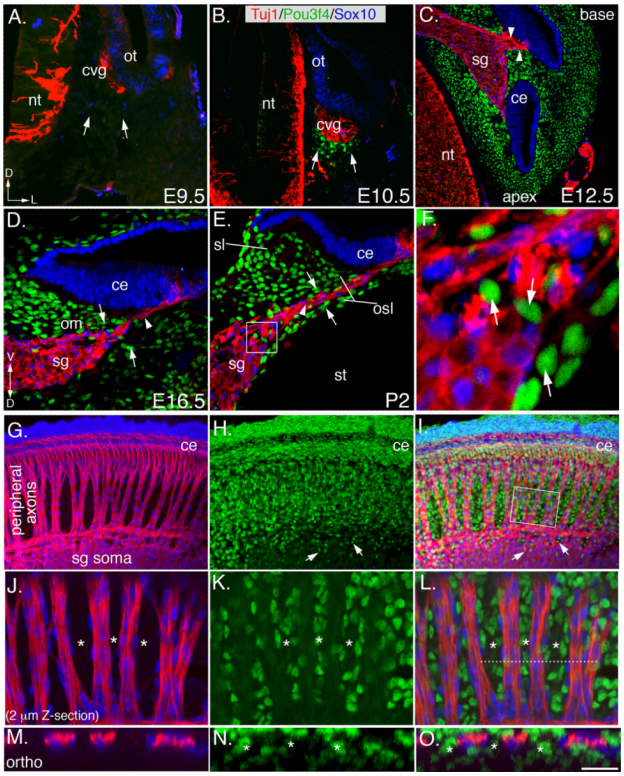

Figure 1. Pou3f4 expression during SGN development in mouse

(A) At E9.5, there is no Pou3f4 expression in the presumptive otic mesenchyme (arrows). nt: neural tube; ot: otocyst; cvg: cochleovestibular ganglion; D: dorsal; L: lateral.

(B) At E10.5, Pou3f4 expression commences in the otic mesenchyme (arrows).

(C) E12.5. At this stage, SGN peripheral axon outgrowth has started (arrowheads) and Pou3f4 protein is expressed by all mesenchyme cells in the otic capsule. sg: spiral ganglion; ce: cochlear epithelium.

(D) Mid-modiolar cross section at E16.5. SGNs peripheral axons (arrowhead) project through otic mesenchyme (arrows) to reach the cochlear epithelium. om: otic mesenchyme. V: ventral.

(E) At P2, SGNs and glia (arrowhead) are clearly separated from the surrounding mesenchyme (arrows). st: scalia tympani; osl: osseous spiral lamina; sl: spiral limbus.

(F) High-magnification image from the boxed region in E. Pou3f4-positive cells (arrows) within the ganglion do not express neuron or glia markers.

(G–I) Whole-mount view of the spiral ganglion and otic mesenchyme at E17.5. Inner radial bundles extend through otic mesenchyme to the cochlear epithelium. Arrows in H and I point to mesenchyme cells analogous to those illustrated in F.

(J–L) A 2 μm thick confocal Z-stack from the boxed region in I illustrates the separation of the axons of the radial bundles and the mesenchyme cells. Asterisks mark bands of mesenchyme.

(M–O) An orthogonal projection derived from the region indicated by the dotted line in L. The asterisks delineate the bands of mesenchyme. Scale bar in O: approximately 150 μm for A–C and G–I; 50 μm for D–E; 10 μm for F; 30 μm for J–L; 20 μm for M–O.

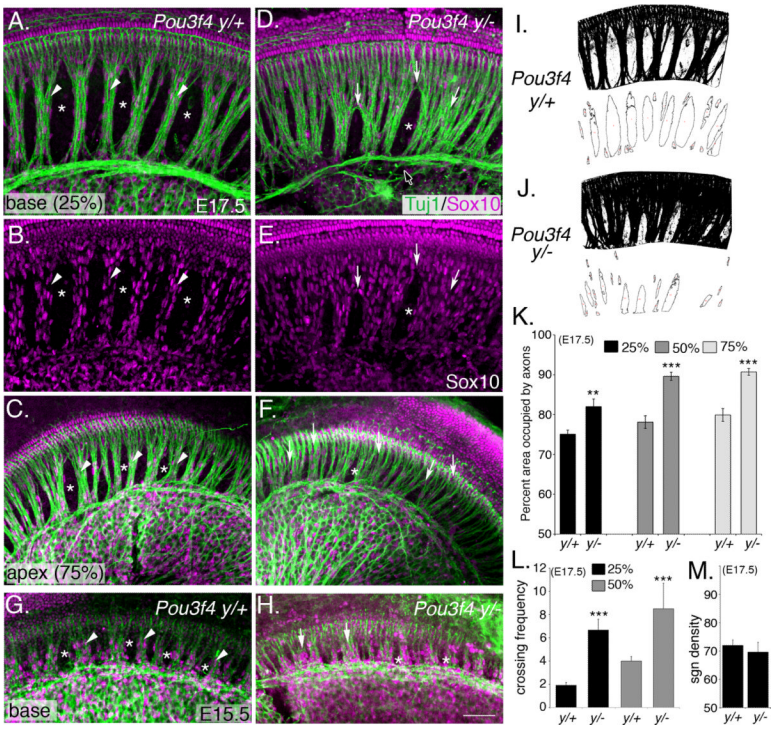

Figure 2. Absence of *Pou3f4* causes defects in fasciculation of inner radial bundles

(A–C) Representative images of the base (A) and apex (C) from a *Pou3f4*$^{y/+}$cochlea at E17.5. Arrowheads point to appropriately formed inner radial bundles; asterisks label bands of otic mesenchyme cells.

(D–F) Whole mount images as in A–C but from *Pou3f4*$^{y/-}$. Arrows point to defasciculated axons. The black arrow (with white stroke) points to the intraganglionic spiral axon bundle (Simmons et al., 2011) that also shows fasciculation defects. As in F, glial cells display a similar ectopic pattern.

(G) At E15.5, the inner radial bundles are apparent (arrowheads), as well as regions of mesenchyme (asterisks).

(H) *Pou3f4*$^{y/-}$ cochlea at E15.5. Fasciculation defects are already evident. Scale bar: 50 μm.

(I–J) Illustration of the scheme by which the radial bundle phenotype was quantified.

(K and L) Histograms illustrating significant increases in axon fasciculation defects (K) and the number of times per 500 μm that individual processes cross between fascicles (L) in *Pou3f4*$^{y/-}$ cochleae. Percentages indicate the position along the length of the cochlea with respect to the distance from the base. **P ≤ 0.01; ***P ≤ 0.001.

(M) The density of neurons along the length of the cochlea is unchanged between *Pou3f4*$^{y/+}$ and *Pou3f4*$^{y/-}$ mice. K–M: mean +/− SEM. Scale bar: 50 −m.

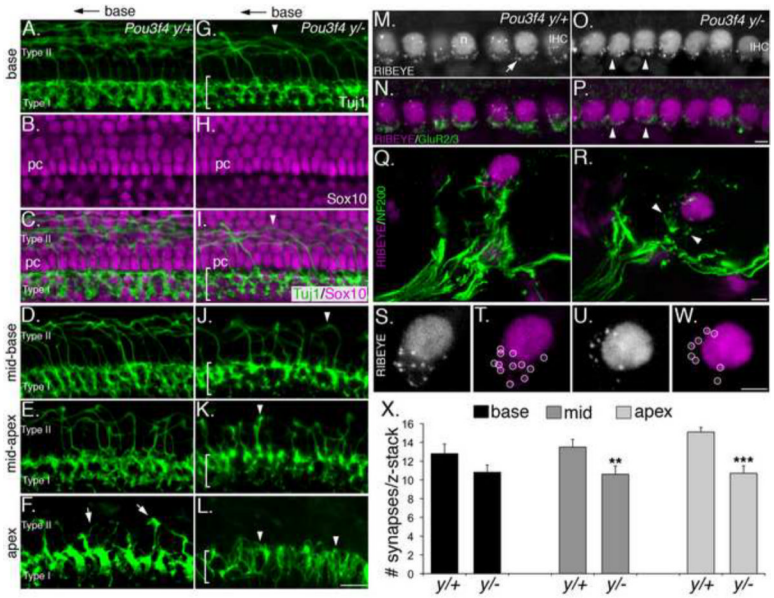

Figure 3. Defects in fasciculation in *Pou3f4*$^{y/-}$ mice impair innervation and synapse formation

(A–L) Type I and Type II projections in *Pou3f4*$^{y/+}$ and *Pou3f4*$^{y/-}$ embryos at E17.5. Only the distal 10 μm of the type I fibers are shown. Scale bar in L = 50 μm

(A–C) At the base of the cochlea, Type I fibers innervate the inner hair cell layer, while Type II fibers cross the pillar cell layer (shown in A and C) and then turn towards the base.

(D–F) Illustration of the base-to-apex gradient of maturation of type II fibers. At E17.5, Type II projections are abundant in the mid-base, sparse in the mid-apex, and short at the apex (arrows).

(G–I) In *Pou3f4*$^{y/-}$ embryos at E17.5, the Type I layer is less dense (see bracketed region), and there are fewer Type II projections (arrowhead).

(J–L) Compared with wild-type, *Pou3f4*$^{y/-}$ embryos show fewer, less mature Type II projections. At the apex (L), no Type II projections are observed. Scale bar = 40 μm.

(M–P) Whole-mount preparation of the apex of *Pou3f4*$^{y/+}$ and *Pou3f4*$^{y/-}$ cochleae at P8. Anti-Ribeye immunostaining indicates ribbon synapses (see arrow in M). This antibody also recognizes CtBp2 (in all hair cell nuclei; n). IHC: inner hair cell. Anti-GluR2/3 (as in N) indicates post-synaptic glutamate receptors. Immunostaining for both factors in the mutant appears reduced (arrowheads).

(Q and R) Mid-modiolar cross-sections of the inner hair cell region from Pou3f4 y/+ (Q) and *Pou3f4*$^{y/-}$ (R) cochleae at E17.5. Nerve terminals are marked by anti-neurofilament (200 kDa). Note the decreased density of nerve fibers contacting the inner hair cell in *Pou3f4*$^{y/-}$(arrowheads).

(S and T) A high-magnification view of the synaptic region from the inner hair cell in Q. Punctate spots (circled in T) represent individual ribbon synapses.

(U and W) Similar view as in S,T but from the *Pou3f4*$^{y/-}$ inner hair cell in R. Note the decreased number of ribbon puncta. Scale bar = 4 μm.

(X) Histogram indicating a significant decrease in the number of inner hair cell synapses (mean +/− SEM) in *Pou3f4*$^{y/-}$ cochleae at P8. **P ≤ 0.01; ***P ≤ 0.001.

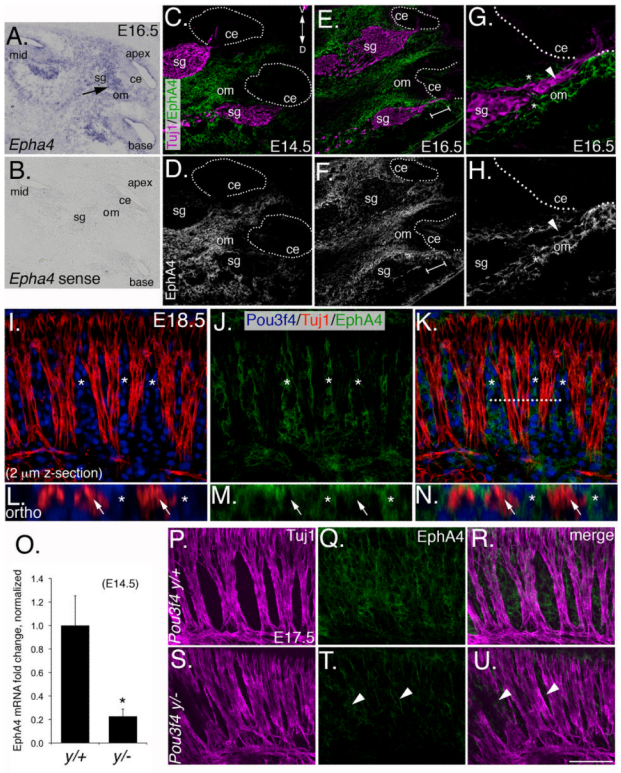

Figure 4. EphA4 is expressed in the otic mesenchyme during development and is decreased in *Pou3f4*$^{y/-}$ embryos

(A and B) *Epha4in situ* hybridization in the E16.5 cochlea. (A) Antisense and (B) sense. Sg, spiral ganglion; om, otic mesenchyme; ce, cochlear epithelium.

(C and D) EphA4 immunostaining at E14.5 Note the absence of EphA4 in all tissues except the otic mesenchyme. The dotted line delineates the cochlear epithelia. D: dorsal; V: ventral.

(E–H) EphA4 immunostaining at E16.5. G and H are a high magnification view from the bracketed region of E and F. Note the “guide rails” marked by the asterisks, and the absence of EphA4 staining in the SGN axons (arrowheads).

(I–K) Whole-mount preparation of a cochlea at E18.5. EphA4 expression is restricted to the mesenchyme (asterisks).

(L–N) Orthogonal confocal reconstructions from the dotted line in K.

(O) Quantitative PCR data showing that *Epha4* expression levels are reduced approximately 5-fold in otic mesenchyme from *Pou3f4*$^{y/-}$ embryos (mean +/− SEM). *P ≤ 0.05.

(P–U). EphA4 expression in wild-type and *Pou3f4*$^{y/-}$ embryos (where it is reduced; see arrowheads) in whole-mount at E17.5. Scale bar: 120 μm for A and B; 100 μM for C–F; 50 μm for G–K; 15 μm for L–N; 70 μm for P–U.

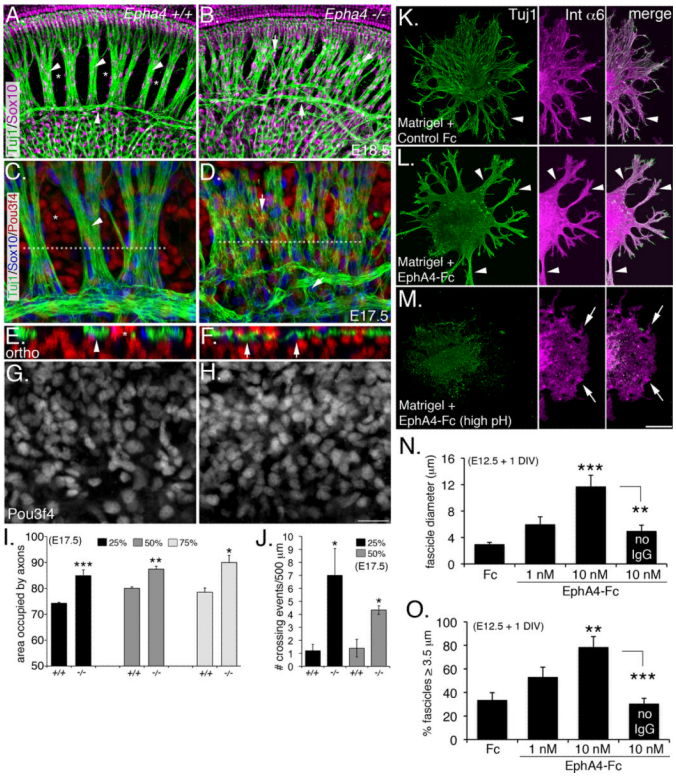

Figure 5. *Epha4*/EphA4 promotes SGN fasciculation and hair cell innervation

(A and B) Wild-type (A) and *Epha4*$^{-/-}$ cochleae (B) at E18.5. Arrowheads in A point to well-defined SGN fascicles and asterisks mark normally formed bands of mesenchyme. In contrast, there is less SGN fasciculation and axons inappropriately traversing the mesenchyme (arrows) in the *Epha4*$^{-/-}$ cochlea (B).

(C and D) High-magnification views of wild-type (C) and *Epha4*$^{-/-}$ cochleae at E17.5 illustrating how the SGNs fail to bundle.

(E and F) Orthogonal reconstructions from the regions marked by dotted lines in C and D showing the SGN bundles and mesenchyme are no longer segregated.

(G and H) Monochrome images indicating no change in Pou3f4 expression in *Epha4*$^{-/-}$ cochleae. (I and J) Histograms illustrating the axon fasciculation defects (I) and the number of times per 500 µm that individual processes crossed between fascicles (J). Percentages indicate the position along the length cochlea with respect to the distance from the base. **P ≤ 0.01; ***P ≤ 0.001. (K and L) E12.5 SGN explants cultured for 24 hours in the presence of Matrigel + Fc control or + EphA4-Fc (both preclustered forms). The middle panels show the auditory glia (Int a6 positive).

(M) Same as L, but the neurons were eliminated using high pH culture medium.

(N and O) Histograms showing increased fascicle diameter (N) and percentage of “large” (≥ 3.5 µm) fascicles in response to EphA4-Fc.**P ≤ 0.01; ***P ≤ 0.001. Scale bars: In H, 50 µm for A and B, 20 µm for B–G; in M, 100 µm for K–M. DIV: days *in vitro*. I,J,N and O, mean +/− SEM.

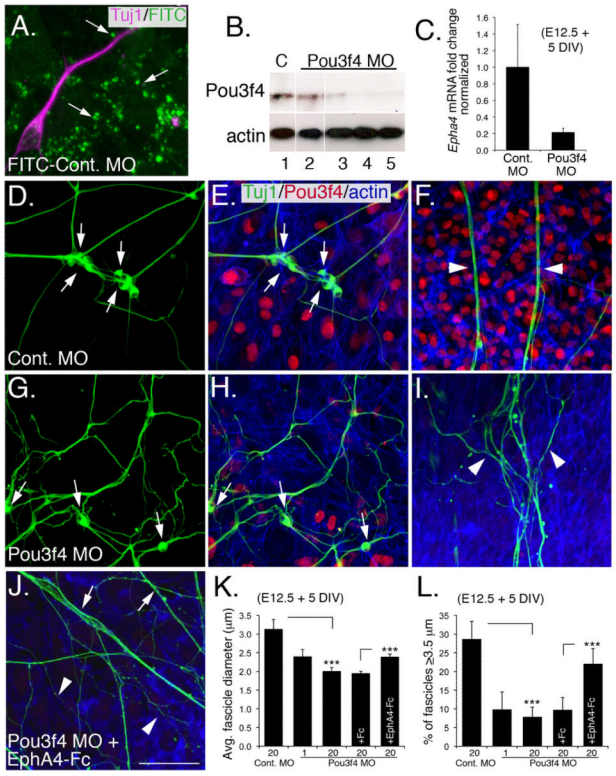

Figure 6. Exogenous EphA4 protein rescues Pou3f4-dependent fasciculation defects *in vitro*

(A) Co-culture of SGNs (magenta) and mesenchyme cells. Punctate FITC-labeling indicates uptake of FITC-conjugated control MO by endocytic vesicles.

(B) Western blot demonstrating knockdown of endogenous Pou3f4 by a Pou3f4 MO. Lane 1: 20 μM control MO; lane 2: 1 μM Pou3F4 MO; lanes 3–5: three different samples treated with 20 μM Pou3f4 MO. Anti-β-actin, loading control.

(C) Quantitative PCR demonstrates a 5-fold reduction of *Epha4* transcripts in mesenchyme cells treated with the Pou3f4 MO. DIV: days *in vitro*.

(D–J) SGN/otic mesenchyme co-cultures treated with indicated MO. Green: anti-Tuj1 (neurons); red: anti-Pou3f4; blue: phalloidin (actin).

(D–F) In the presence of 20 μM control MO, SGN cell bodies cluster (arrows in D,E) and have axons that form thick, straight fascicles that extend away from the cell bodies (arrowheads in F).

(G–I) Treatment with 20 μM Pou3f4 MO decreases clustering of cell bodies (arrows in G,H), as well as decreased axon fasciculation (arrowheads in I). In addition, individual fibers follow more convoluted paths. Knock down of Pou3f4 is illustrated in (H).

(J) Treatment with 20 μM Pou3f4 MO + 10 nM EphA4-Fc increases incidences of thick, straight fascicles (arrows) although single non-fasciculated neurites are still present (arrowheads). Scale bar: 20 μm for A; 40 μm for D–J.

(K,L) Histograms illustrating changes in average fascicle diameter (μm) and average percentage of “large” ≥ 3.5 μm fascicles among the different treatment groups. ***P ≤ 0.001. C,K, and L, mean +/- SEM.

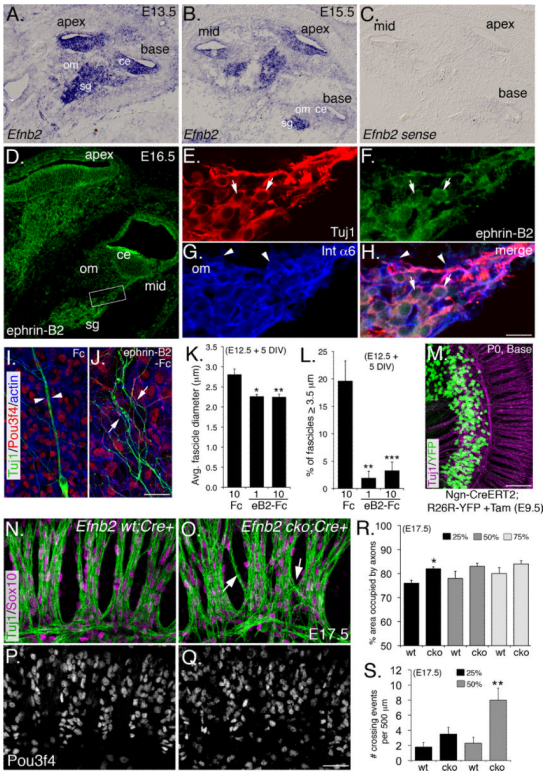

Figure 7. Ephrin-B2 acts as a cofactor for EphA4 during SGN fasciculation

(A–C) *Efnb2 in situ* hybridization at E13.5 and E15.5. sg: spiral ganglion; ce: cochlear epithelium; om: otic mesenchyme.

(D) Ephrin-B2 antibody staining of the cochlea at E16.5.

(E–H) High magnification view from the boxed region in D. (E) SGNs. (F) Ephrin-B2 expression primarily in the neurons (see arrows). (G) Glial cells (see arrowheads). (H) Merge. (I and J) Representative control Fc and ephrin-B2-Fc-treated samples from SGN/otic mesenchyme cultures. See text for details.

(K and L) Histograms showing decreased average fascicle diameter (K) and percentage of "large" fascicles (L) in the presence of blocking ephrin-B2-Fc. DIV: days *in vitro.*

(M) Tamoxifen induction of Ngn-Cre^{ERT2} induces expression of YFP reporter activity in ~95–100% of SGNs (see Experimental Procedures).

(N) Micrograph showing morphology of the radial bundles in a control *Efnb2 wt; Cre+* cochlea.

(O) Micrograph showing less fasciculation and processes crossing between bundles (arrows) in *Efnb2 cko; Cre+* cochlea.

(P and Q) Pou3f4 staining shows that mesenchyme is normal in both *wt* and *Efnb2 cko* cochleae.

(R and S) Histograms illustrating axon fasciculation defects (R) and the number of times per 500 μm that individual processes crossed between fascicles (S). Percentages indicate the position along the length cochlea with respect to the distance from the base. *P ≤ 0.05; **P ≤ 0.01. Scale bars: in H, 200 μm for A–C, 100 μm for D, 20 μm for E–H; in J 40 μm for I and J; in M, 80 μm; in R, 40 μm. K,L,R and S, mean +/- SEM.

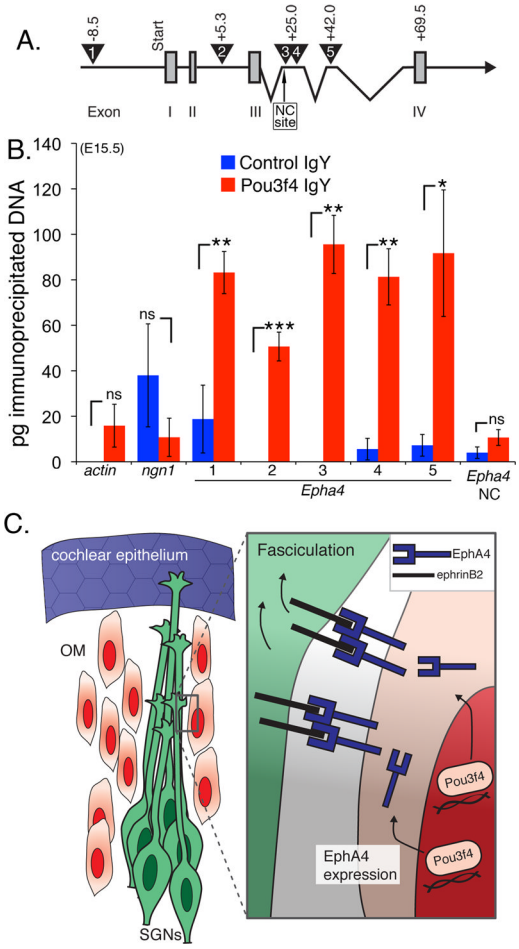

Figure 8. Pou3f4 protein associates with *Epha4* regulatory elements

(A) A cartoon schematic of *Epha4* showing the first four of 16 exons. Exons I–IV (numbered gray boxes). The numbered triangles indicate the regions containing the putative Pou3f4 binding site ATTATTA. Primer sets were designed to amplify these five regions after ChIP. The negative control site, "NC site."

(B) Histogram showing the number of picograms (pg) of immunoprecipitated chomatin for each primer set. ns = not significant. *P ≤ 0.05; **P ≤ 0.01; ***P ≤ 0.001. Mean +/- SEM.

(C) Cartoon schematic of a proposed model. Pou3f4 in otic mesenchyme induces expression of *Epha4*/EphA4, which binds to ephrin-B2 on developing SGN axons leading to fasciculation. As a result, SGN axons fasciculate to give rise to the inner radial bundles.